

Nuclear Magnetic Resonance

Author: James Dragan

Lab Partner: Stefan Evans

Physics Department, Stony Brook University, Stony Brook, NY 11794.

(Dated: December 5, 2013)

We study the principles behind Nuclear Magnetic Resonance using a TeachSpin pulsed Nuclear Magnetic Resonance (pNMR). We measured relaxation times (T_1 , T_2 , T_2') of hydrogen in liquid samples, with chemical composition containing hydrocarbons, by rotating the samples nuclear spin, through various methods, and measuring the time it takes the spins to equilibrate. Equilibrium is defined by the direction of a permanent magnetic field. This procedure in this lab can be used to determine the chemical composition of any random sample if there are known values for different samples.

1. INTRODUCTION

Widely used in many fields of science, Nuclear Magnetic Resonance (NMR) has the ability to characterize samples. The most notable application of magnetic resonance is a Magnetic Resonance Imaging (MRI) machine which is heavily used in the medical field and widely known throughout the public. The ability for NMR to measure local magnetic fields in atomic nuclei make it much better than an ordinary magnetometer, which measures average field.

NMR is based off the principles of magnetic resonance. When a charged particle (in our case: protons) is in the presence of a magnetic field, the particle experiences a torque. Thus the particle is given angular momentum and precession occurs around the magnetic field (z-direction). When an external field is applied, resonance conditions can be applied such that the particle processes - in the x-y plane - around its original axis of field orientation - z-axis. Resonance occurs when the applied field is of the same frequency as the frequency of the particle's precession in the perpendicular plane to the static magnetic field. The external field, in this case is a pulse of radio frequency (rf). From quantum mechanics we know that there are discrete energy levels corresponding to the spin of a particle around a static magnetic field, B_0 . These energy levels are spaced by $\Delta E = \hbar\gamma B_0$ where $\gamma = \mu/J\hbar$, is the gyromagnetic ratio and J is the spin of the nucleus. The frequency of precession is given by the Lamour frequency,

$$\omega_L = \gamma B_0. \tag{1}$$

It should be noted here that we are dealing with elements that are spherically symmetric with respects to the electron distribution. This is why we concern ourselves with the nuclear spin, otherwise the nuclear spin would be a small perturbation on the total spin of the atomic sample. In this experiment to have a signal of detectable magnitude we deal with samples that are proton abundant. These samples will give a strong NMR signal.

By applying resonance conditions in terms of an rf pulse, we are able to flip the spin's projection from the z-axis to the x-y plane. Once flipped, the particle will precess around the z-axis at the Lamour frequency, if the applied frequency is on resonance. Because we have a moving charged particle, the particle will give off an EMF which can be detected by a pick-up coil.

When the rf pulse is applied, energy is given to the system. The spin states, who want to return back to the equilibrium - spin orientated along the z-axis - will exchange thermal energy with each other until they return back to the z-axis. Due to the inhomogeneous field of the permanent

magnet, B_0 , different spin-states, after being rotated to the x-y plane, will begin precessing with different angular velocities because they observe different magnetic fields. Once the spin-states exchange energy they align back to the z-axis, there will be no EMF detected by the pick-up coil and thus our signal decreases to zero. The time it takes for the spin states to go back to equilibrium is called the relaxation time. The next section will discuss the evolution of the spin-states for three different pulse schemes.

2. PROCEDURE

It is first important to understand the two types of rf pulses applied produced by the TeachSpin pulsed NMR. We define that the permanent magnetic field in this system produced the permanent magnet is orientated in the +z direction. The magnetic field produced, B_0 , can be varied by changing the applied current. From the TeachSpin pNMR, a $\pi/2$ pulse, referred to as an A pulse, will temporarily flip the net magnetization of the spins to the x-y plane if the frequency of the rf field is resonant. A π pulse, referred to as a B pulse, will temporarily flip the net magnetization to the -z-direction assuming the spin states were originally aligned in the z-axis. This can be pictured on a sphere, defined as the Bloch sphere, with the north and south poles corresponding to spins aligned in the z-axis and -z - axis respectively, and spins aligned along the equator are in the x-y plane. Thus a $\pi/2$ pulse will move spins originally from the north pole (z-axis) to the equator (x-y plane) and a π will orient the spins from the north pole to the south pole.

When used together in three distinct orders (P π then $\pi/2$ or $\pi/2$ then π pulse) we can measure the three relaxation times which are defined in the following three sections. As described above we can use A. Bloch's equations^[1] to describe the evolution of the system of spin states by viewing them on the Bloch sphere. These solutions are completely analogous to the evolution of a two-level energy state system of an atom under a time-dependent potential (i.e. atomic interaction with lasers). Equations 2,3 and 4 represent the evolution of the spin-state system (not individual spin-states) after an applied $\pi/2$ pulse.

$$\frac{dM_z}{dt} = \frac{M_0 - M_z}{T_1} \quad (2)$$

$$\frac{dM_x}{dt} = \frac{M_x}{T_2} \quad (3)$$

$$\frac{dM_y}{dt} = \frac{-M_y}{T_2} \quad (4)$$

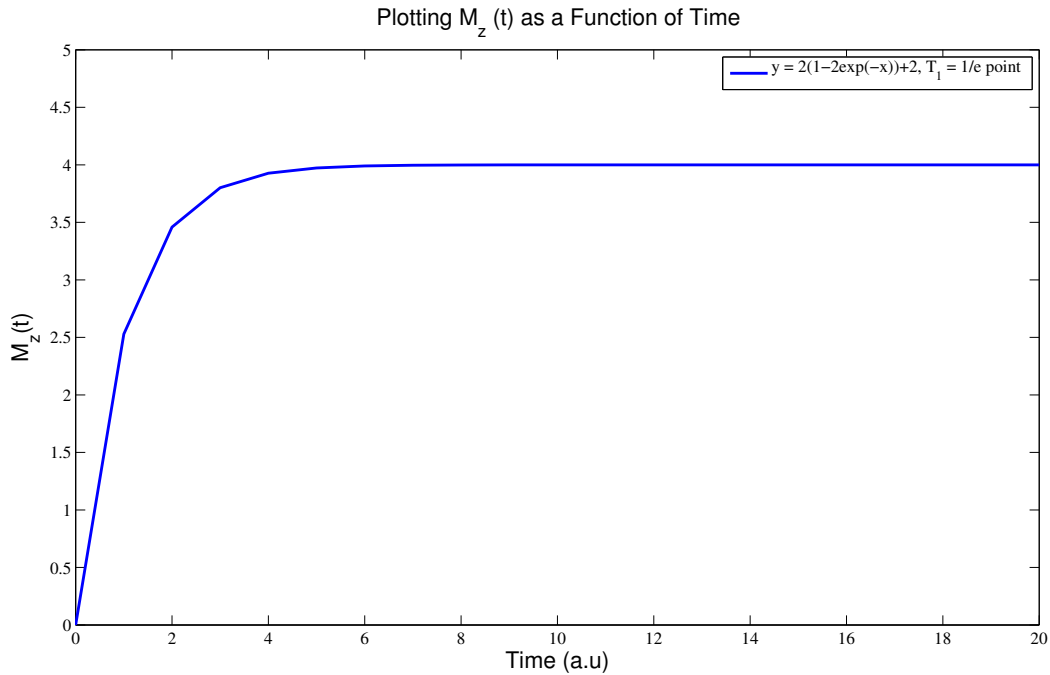
As explained previously, the spin-state system will return back to equilibrium after some time through exchange of thermal energy. It is the time taken to return to equilibrium, that corresponds to various pulse orders, that is defined below.

2.1. Spin-Lattice Relaxation Time: T_1

Solving Eq. (2) can be easily found by integrating and using the boundary condition that $M_z(t = 0) = 0$ we find that

$$M_z(t) = M_0(1 - 2e^{-t/T_1}) \quad (5)$$

where T_1 is the spin-lattice relaxation rate and is shown graphically below.



This value is measured by applying a π pulse to flip the spin to the $-z$ -direction. At a time t after the π pulse is applied a $\pi/2$ pulse is applied. By varying the time between the two pulses we can measure T_1 . This can be understood conceptually as we increase t . If the $\pi/2$ pulse is

applied immediately after the π pulse, the all the states will be rotated to the x-y plane, thus we see a local maximum as we observe the amplitude in the pick-up EMF signal. If we increase t then we allow more time for the spins to begin relaxing so when the $\pi/2$ pulse is applied not all the spin states will rotated to the x-y plane thus our detected signal will decrease. At a certain time t the spin states will have relaxed to the x-y plane, then by applying an A pulse the spin-states are then oriented to the z-axis, and no signal is detected. At a later time the spin-state will have relaxed past the x-y plane towards the z-axis, so if an A pulse is applied then these states will flip past the z-axis into some orientation of the spin containing all three components, meaning there is precession that the pick-up coil will detected. At an even greater time, all the spins have had enough time to relax back to their equilibrium state, which we define as the z-axis, then an A pulse will strictly orient them to the x-y plane and we observe another maximum in the detected signal. Here the maximum hits an asymptote since so much time has passed the spin state are back at equilibrium and until an A pulse is applied, the spin-states will remain oriented there.

As we vary t between the two pulses we can determine T_1 by recording the amplitude of the signal at each time step. T_1 can also be used to determine T_2 using the following equation:

$$\frac{1}{T_2} = \frac{1}{T_2^*} + \frac{1}{T_2'} \quad (6)$$

where,

$$\frac{1}{T_2'} = \frac{1}{T_2''} + \frac{1}{2T_1} \quad (7)$$

Here, T_2 is the Free Induction Decay (FID), T_2^* is the relaxation due to the inhomogeneous B field (B_0), T_2' is the spin echo decay, and T_2'' is the relaxation due to the spin-spin interaction.

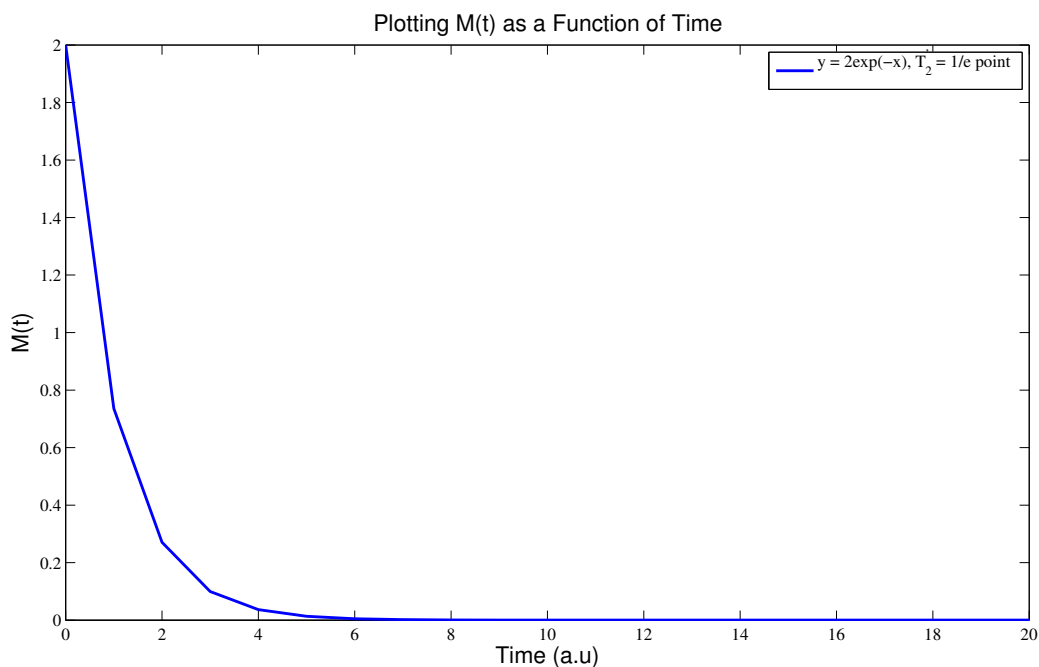
2.2. Spin-Echo Decay: T_2'

This spin echo decay is a relaxation rate that includes interactions between spin-states (T_2'') to effect the total relaxation time. In liquids we find $T_2'' \ll 2T_1$ and we neglect this term, for solids this is not the case. In this limit, from Eq. (7), we find that

$$T_2' = 2T_2. \quad (8)$$

By measuring this rate, we can eliminate unwanted effects of magnetic field inhomogeneities. This can be measured by applying a single $\pi/2$ pulse followed by a series of π pulses. The resulting decay of detected signal can be understood by the following function of τ which is the time between the two pulses.

$$M_{echo}(\tau) = M(0)e^{-\tau/T_2'} \quad (9)$$



The application of the initial $\pi/2$ pulse will orient the spins to the x-y plane as described. Due to the inhomogeneous magnetic field, different protons see different fields and thus precess at different rates. The inhomogeneity causes a range of precessions centered at some average rate. By applying a π pulse the spins are allowed to regroup before dephasing again. After the π pulse is applied the spins that now were 'ahead' of the average are behind, and those that were 'behind' the average are now ahead resulting in all the protons to catch up to the average or rephase. After, the spins begin to dephase again. This is apparent by observing a maximum on the oscilloscope after the application of a π pulse then a decrease in signal as the spins dephase. The procedure done to determine T_2' was to applying a series of Pi pulses (on the order of tens of pulses) after the initial $\pi/2$ pulse. In this way we observed the rise and fall of many maximas of an amplitude

that would decay. By recording each maxima in time and then plotting those points T'_2 can be determined.

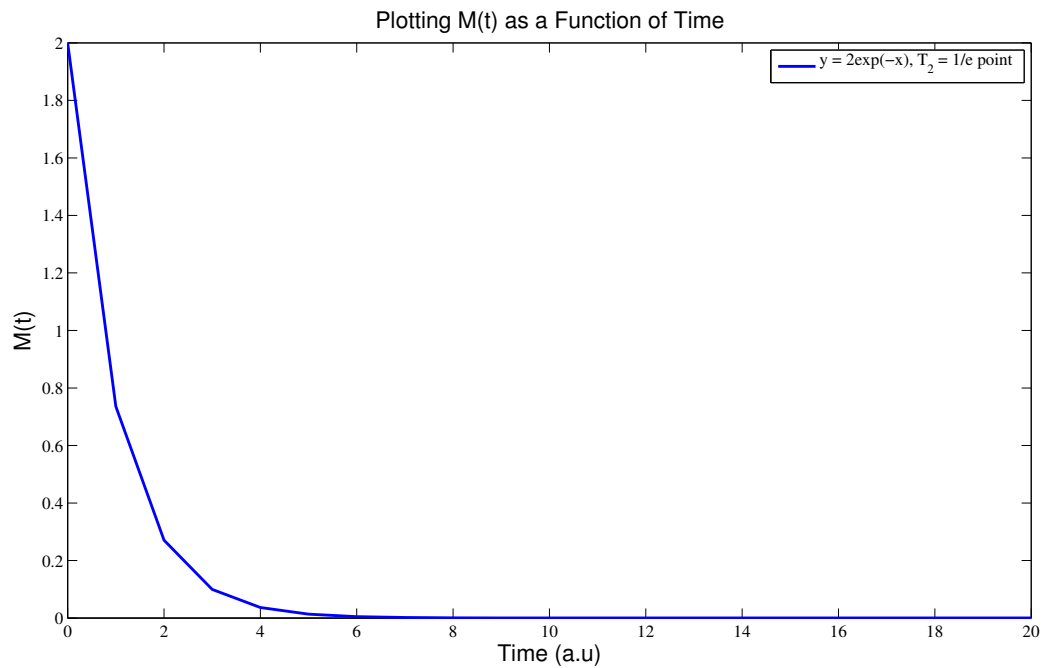
Another procedure to determine T'_2 , which was not done in this lab, is to vary the time between the A and B pulses and to plot the the maximum as a function of time. Although not done, this result should be the same as the result found from the procedure described in the paragraph above.

2.3. Free Induction Decay (FID): T_2

We see that T_2 is defined by Eq. (6). The Free Induction Decay (FID) is characteristic of the spin-states angular velocities. By applying one $\pi/2$ pulse we can measure T_2 . We know that once in the x-y plane, different protons will be influenced by different magnetic fields due to the inhomogeneity of the permanent magnetic. Thus different protons will precess at different rates around the z-axis which we defined as dephasing. In the process of dephasing the spin-states exchange thermal energy within the system. This exchange of thermal energy causes the spin-states to return to equilibrium causing the detected signal on the oscilloscope go from a maximum after the $\pi/2$ pulse is applied to zero. The time it takes for the signal to decay to zero is the Free Induction Decay time.

Measurements are done by fitting the data to the solution of Eq. (4). The solution is given as,

$$M(t) = M_0 e^{-t/T_2}. \quad (10)$$



2.4. Experimental Set Up

To detect these parameters of a given sample a pNMR spectrometer from TeachSpin is used. Samples in small vials are placed in the center of the permanent magnetic. When measuring T_1 , T_2^* and T_2' the same procedure was applied for all samples. A diagram of the set up is shown below.

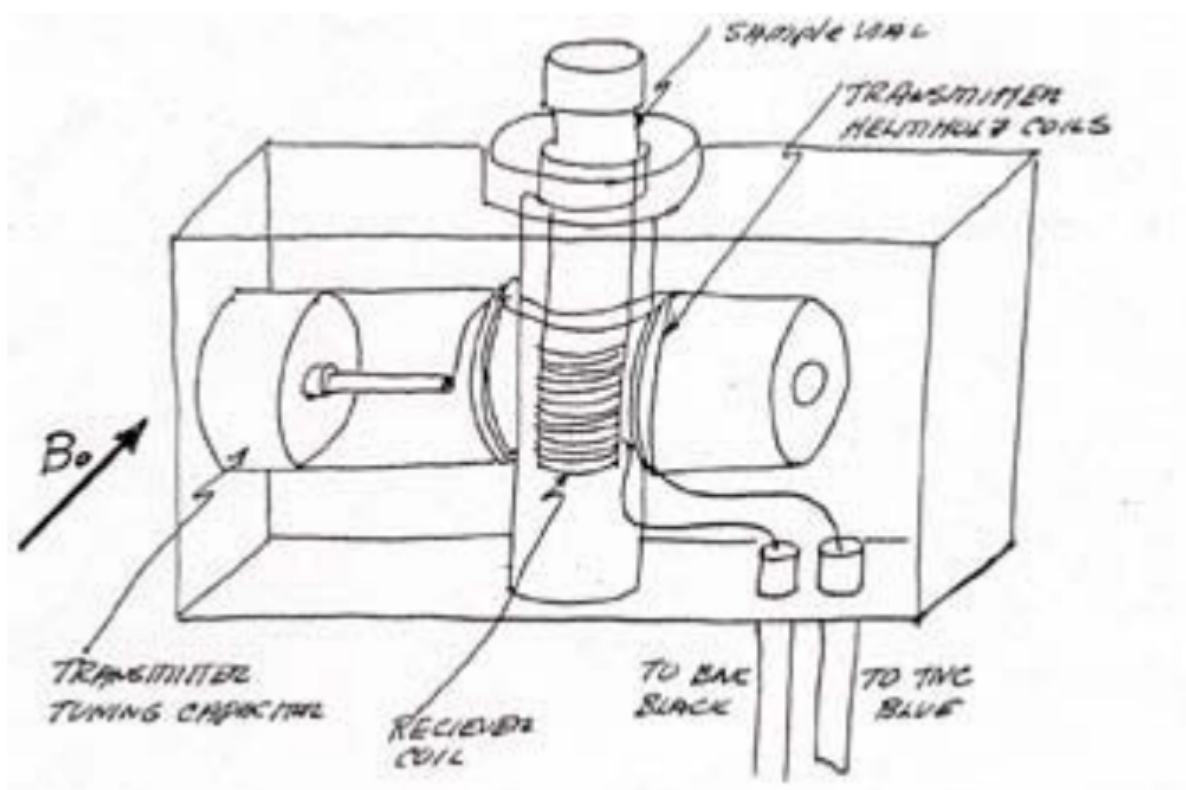


FIG. 1: A 3-d view of the pNMR apparatus is shown^[2]. The receiver coil is oriented such a way as to detect only the EMF given by the precessing protons.

The sample has its protons spins aligned with B_0 . By the application of the rf pulse, spins are oriented in either the x-y plane from a $\pi/2$ pulse or are in the z or -z direction depending on their original state by the application of a π pulse. As the spins precess, the resulting EMF is detected by the receiver coils and sent to the oscilloscope. The circuit diagram for this set up is shown below. It shows the path taken by the rf pulse and the received signal.

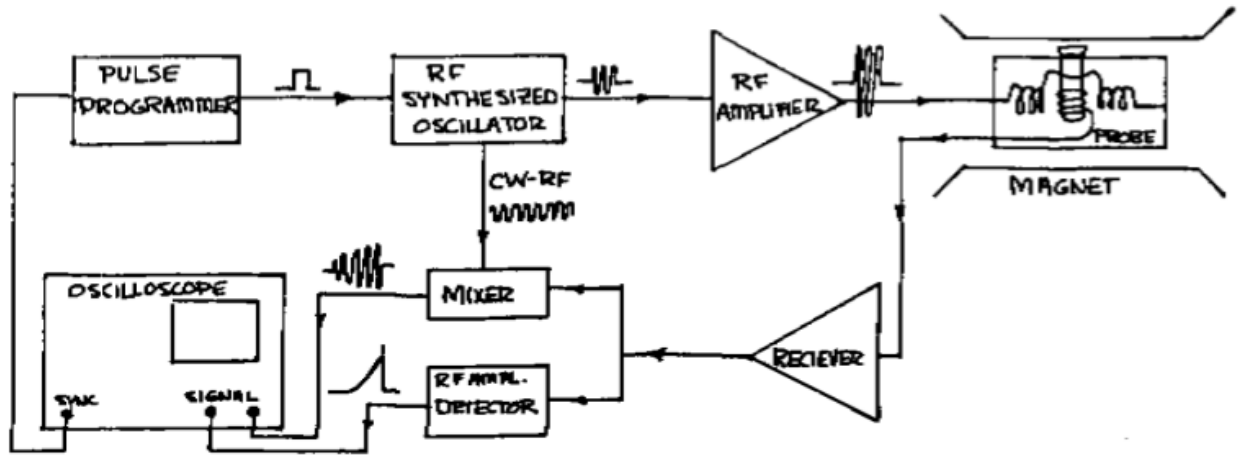


FIG. 2: A diagram following the several signals in this experiment is shown^[3].

Resonance was found applying a $\pi/2$ pulse and changing the current applied to the permanent magnetic field, B_0 , such that the detected signal was maximized. Then the frequency was adjusted so that the mixed signal - a beat of both the rf and received signal - was minimized to a signal peak, or a flat line. At resonance, if the width of the A pulse was increased to that of a π pulse, we observed no FID detected signal verifying resonance. It was also done by observing the beat frequency between the detected signal and the original rf frequency. On resonance, since the two frequencies should be the same, then there is no detected beat. By observing the beat signal decrease to zero we could also determine resonance conditions. By following the procedures in Section [2] we can then measure the various relaxation times.

3. DATA AND ANALYSIS

In all the analysis, Matlab was used to extract the raw data and process it. In processing we used three different fitting functions, corresponding to T_1 , T_2 and T_2' respectively. We determine the "goodness" of our fit by obtaining a Reduced χ^2 that is close to 1. The formula for the Reduced χ^2 is given by^[4],

$$\text{Reduced } \chi^2 = \frac{\sum_1^N \frac{(y-f(x))^2}{\sigma^2}}{N - \nu} \quad (11)$$

where N is the number of data points, y is the measured value, f(x) is the fitted value, σ is the error and ν is the number of free parameters (three in this case of all fitting functions). The error

σ was estimated by observing the average distance between the fit curve and the measured values.

We measured T_1, T_2 and T_2' for the following samples: Mineral Oil, Paraffin Oil, and an Unknown Sample. In addition we also measured T_1, T_2 and T_2' for four concentrations of $\text{Fe}(\text{NO}_3)_3$ in water. In the following sections examples of the data and fitting functions are shown for mineral oil. The graphs and fitting functions for all of the samples measured can be found in the Appendix.

It should be noted that the resonance frequencies are not mentioned because of drifts in the voltage to the permeant magnetic field. The same sample will have its resonance condition drift over the course of hours, making day to day resonance conditions incomparable. Despite this the overall measurements of the relaxation times did not change (as one would suspect) day to day, which is not shown in this lab but was verified by the experimenters.

In addition, while the magnetization is a free parameter, the value found does not pertain to the true magnetization of the sample. This is due to the procedure in which we measured the relaxation times as well as editing done in the data analysis. Our focus was measuring the relaxation times as stated and therefore the procedure followed the focus.

3.1. T_1

The procedure to determine T_1 is described in Section [2]. We find that by increasing the delay between the B and A pulse the signal goes from a maximum to a minimum and back towards an asymptote corresponding to the magnetization of the sample. This is shown mathematically below and was the fitting function used.

$$M_z(t) = M(1 - 2e^{-t/T_1}). \quad (12)$$

Below are our measured results for both mineral oil.

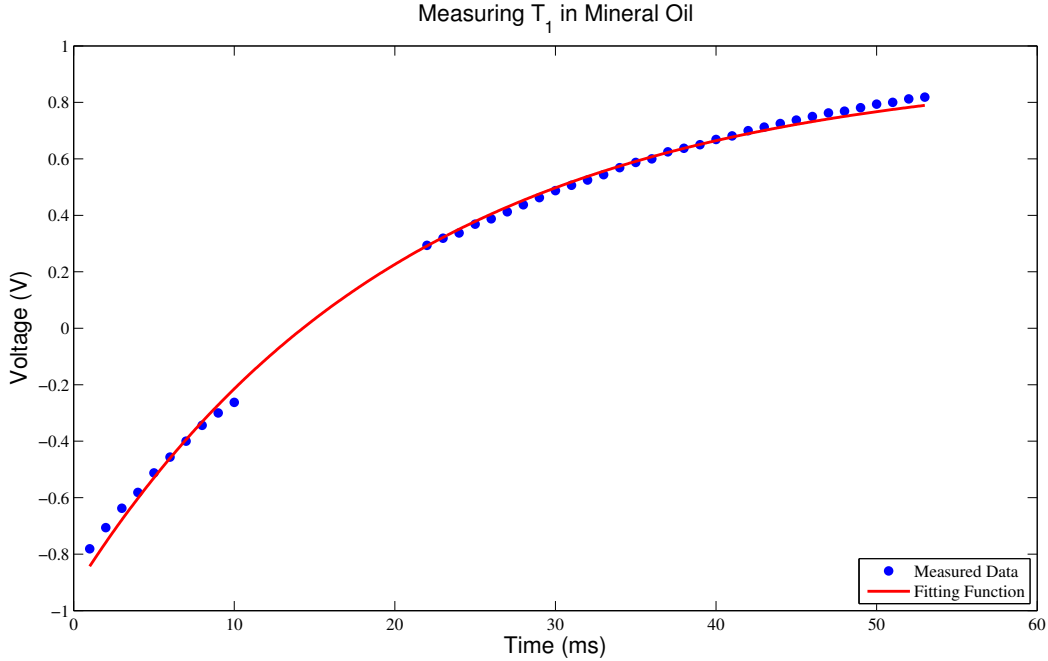


FIG. 3: Here the beginning set of points were reflected over the x-axis to get an exponential curve that hits an asymptote. This procedure is done for all the following measurements of T_1 . Our fitting function gave $T_1 = 20.59 \pm 0.36$ ms, with error = $\sigma = 0.02$ and a Reduced $\chi^2 = 1.0177$

To have improved the accuracy of this result, more data points near the asymptote should have been taken. Points near $V = 0$ are removed because of the noise of the signal, where maximums were measured that were not actual maximums of the signal.

The found values of T_1 for the other samples can be found below in Section [3.4].

3.2. T_2

As described in Section [2], once resonance was found we sent an A ($\pi/2$) pulse to the sample, orienting the spins in the x-y plane. By measuring the decay of the signal we measure the Free Induction Decay (FID). The following fitting function was used.

$$M(t) = M_0 e^{-t/T_2} \quad (13)$$

Below is a graph showing our measurement of T_2 for mineral oil.

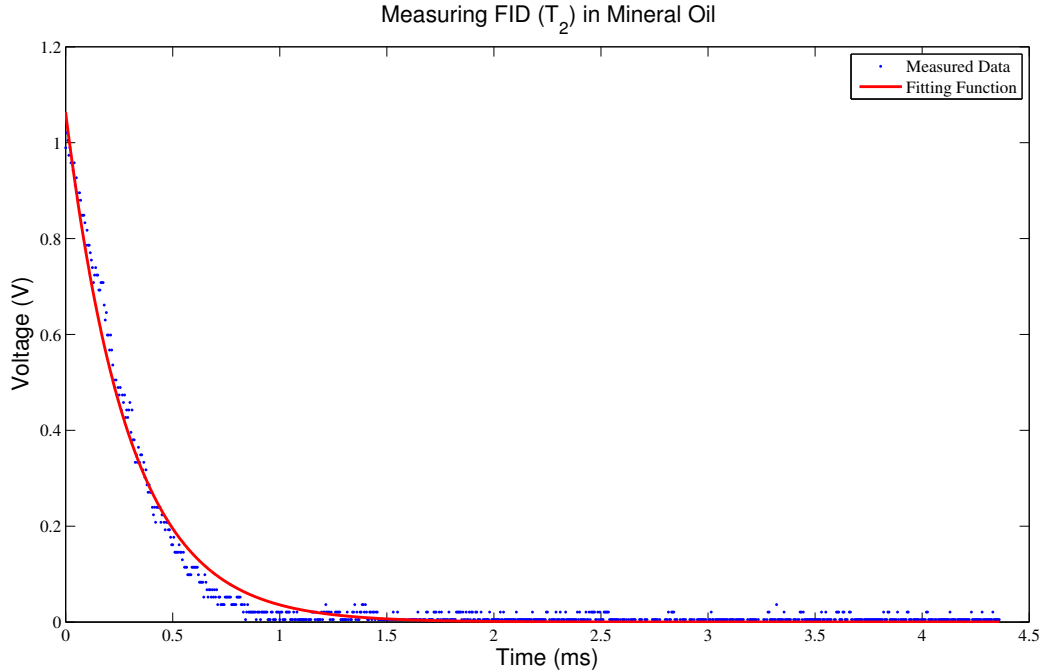


FIG. 4: The FID of mineral oil is shown. Note the measured data does not hit zero due to noise in the electronics.

We found T_2 to be 0.2949 ± 0.004 ms from a fitting function of $\sigma = 0.023$ and reduced $\chi^2 = 1.0308$.

The values of T_2 for the other samples can be found below in Section [3.4].

3.3. T'_2

We expect that the spin-echo decay time (T'_2) be longer than the FID. This is because the spin's are constantly being flipped by a series of B pulses followed by a single A pulse whereas in the FID only a single A pulse acts on the sample. In the case of the spin-echo decay the constant application of a B pulse does not allow different spins to align together, because they are not given the time to. This means they have less time to exchange thermal energy causing their rotation back to the z-direction, and thus equilibrium, to take longer. This is verified by our data shown in Section [3.4]

The following function was used to fit the data,

$$M(t) = M_0 e^{-t/T_2} \quad (14)$$

Below are our measured results for mineral oil.

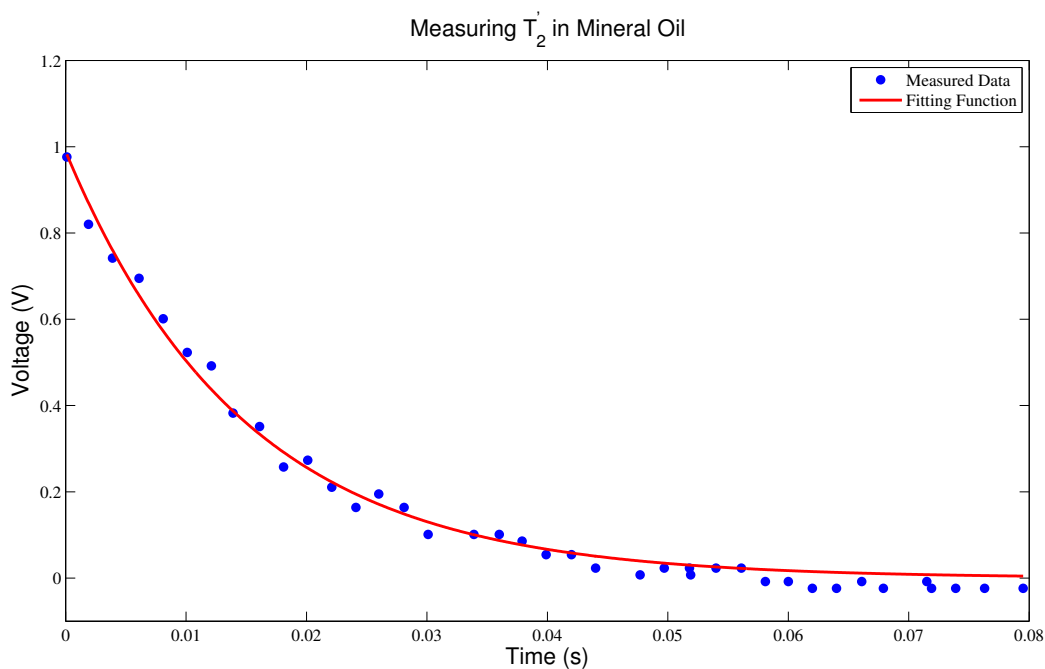


FIG. 5: The spin-echo decay for mineral oil.

Our fitting function returned a value of $T_2' = 14.83 \pm 0.78$ ms for a $\sigma = 0.025$ and reduced $\chi^2 = 1.0915$. We do indeed note that this relaxation time is longer than the FID for mineral oil.

We will now look at these values for each sample tested and discuss.

3.4. Summary and Correlations

Following the same procedure described above we measured the following values for each of our seven samples. For simplicity, samples of different concentrations such as 0.05M of $\text{Fe}(\text{NO}_3)_3$ in water is written as 0.05M.

Sample	T_1 (ms)	T_2' (ms)	T_2 (ms)	T^* (ms)
Mineral Oil	20.59 ± 0.36	14.83 ± 0.78	$.2949 \pm 0.004$	0.3 ± 0.031
Paraffin Oil	31.11 ± 0.93	13.57 ± 0.2	0.4039 ± 0.0063	0.41 ± 0.012
Unknown Sample	21.17 ± 1.24	11.14 ± 0.3	0.4379 ± 0.0038	0.45 ± 0.024
0.05M	2.07 ± 0.118	1.389 ± 0.06	0.3992 ± 0.0039	0.56 ± 0.048
0.075M	0.6307 ± 0.0064	0.4266 ± 0.0562	0.3653 ± 0.0021	2.54 ± 0.669
0.1M	0.4116 ± 0.0065	0.4989 ± 0.0277	0.3813 ± 0.0025	1.61 ± 0.179
1.0M	0.06438 ± 0.00429	0.4116 ± 0.0247	0.3456 ± 0.0027	2.15 ± 0.258

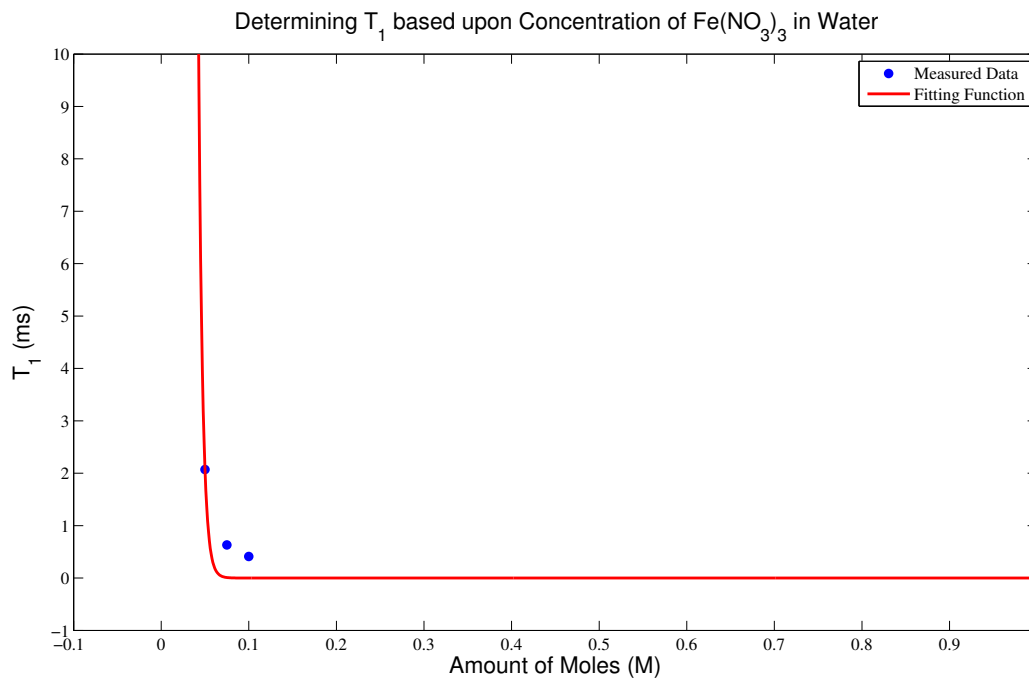
The first thing to note is that, the unknown sample - which was originally believed to be another concentration of $\text{Fe}(\text{NO}_3)_3$ - is probably paraffin oil with water or something close in chemical composition. It may be paraffin oil, but with a smaller volume than the known vial of paraffin oil resulting in the shorter relaxation times. This sample indicates the power of NMR as a tool for characterizing samples. We immediately thought the unknown sample was a concentration of $\text{Fe}(\text{NO}_3)_3$ but from the analysis we could immediately rule that off by testing several other concentrations of $\text{Fe}(\text{NO}_3)_3$ in water.

Using the Eq. (6) we estimated T^* , which is the relaxation due to the inhomogeneous magnetic field, for each sample shown. Theoretically this should be the same regardless of sample but we find that this is not the case. It may be that different samples see a different inhomogeneous field as a result of their own atomic properties. It could also be a byproduct of stray magnetic fields from the laboratory, which are hardly consistent.

It is also interesting to note that T_1 and T_2' do not relate corresponding to Eq. (8). In fact for the first three samples - mineral oil, paraffin oil, and the unknown - it appears that $T_1 \simeq 2T_2'$. This is a testament to the experimental errors including the DC drift in the permanent magnet.

Using this table, we can make a rough estimate for a function relating T_1 , T_2' , T_2 to different concentrations of $\text{Fe}(\text{NO}_3)_3$ in water. This is shown below. Again, Matlab was used to fit to the data points and provided a 'goodness' of fit described by Eq. (11). For all three of these graphs a boundary condition of $T(0) = 100,000$ was chosen in accordance with the trends of the graphs where the relaxation time appear to diverge to infinity if the amount of concentration was zero. It would make sense intuitively for the relaxation time to either be 0 or infinity for a concentration of pure water making the relaxation time 0 or infinity. Following for each relaxation time 0.05M of $\text{Fe}(\text{NO}_3)_3$ had a greater value than the other it would make little physical sense that even less concentrations would have a weaker relaxation time. Thus the boundary condition was chosen to

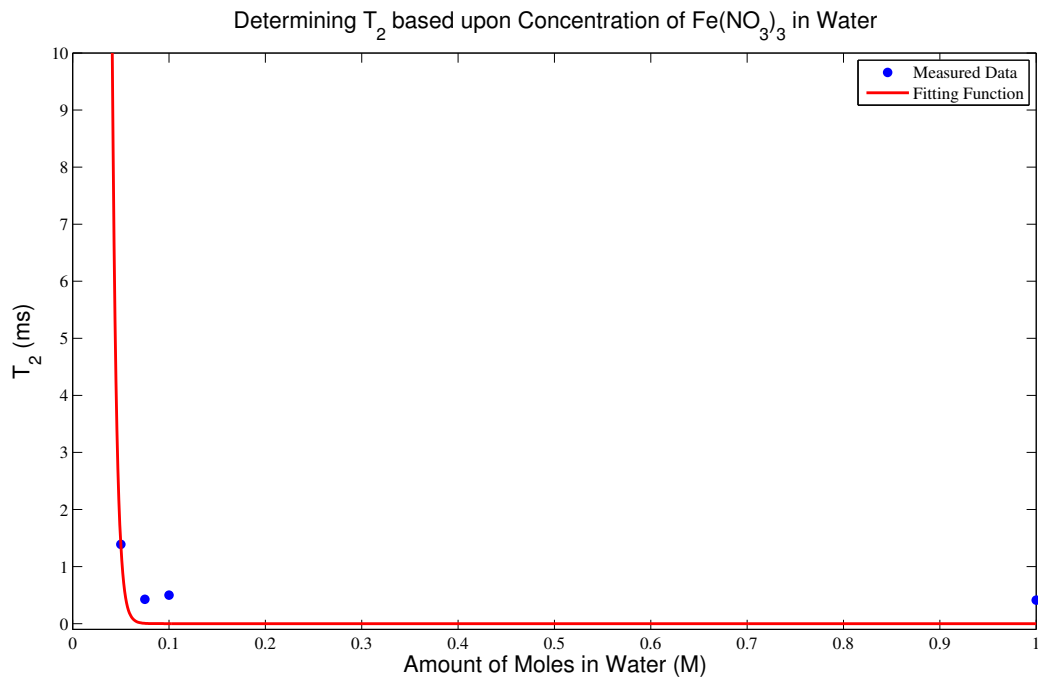
represent "infinity" but allowed a return of actual values from the Matlab code.



The fitting function used here is given by,

$$T_1(M) = Ae^{-M/B} \quad (15)$$

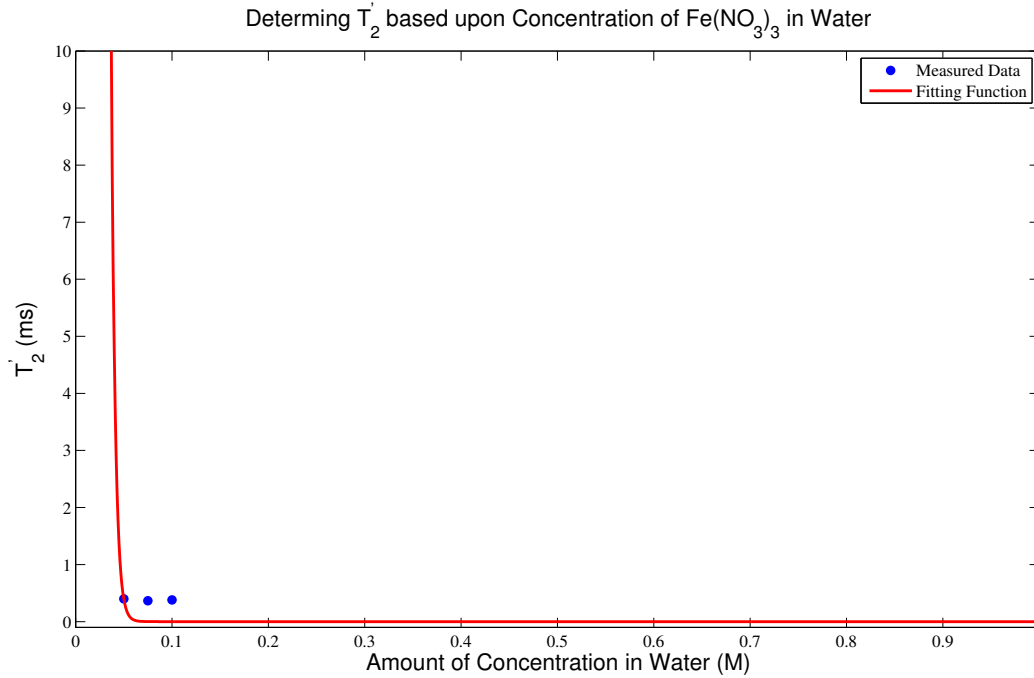
where $A = 10^5 \pm 10^4$ ms and $B = 0.004637 \pm 0.000285$ M for $T_1(M)$. The fit had an error of 0.35 and a reduced $\chi^2 = 1.52$



The fitting function used here is given by

$$T_2(M) = Ae^{-M/B} \quad (16)$$

where $A = 10^5 \pm 10^4$ ms and $B = 0.004471 \pm 0.000407$ M for $T_2(M)$. The fit had an error of 0.4 and a reduced $\chi^2 = 1.24$



The fitting function used here is given by

$$T_2'(M) = Ae^{-M/B} \quad (17)$$

where $A = 10^5 \pm 10^4$ ms and $B = 0.004023 \pm 0.000937$ M for $T_1(M)$. The fit had an error of 0.3 and a reduced $\chi^2 = 1.47$

The large error in these data points is a result of having just one more data point than free parameters. If this experiment were to be repeated, more concentrations of $\text{Fe}(\text{NO}_3)_3$ in water would be tested to obtain a better fit. The graphs are intuitive by looking at if $M \rightarrow 0$, we expect the relaxation time to diverge to infinity. In addition if there were so many $\text{Fe}(\text{NO}_3)_3$ particles to flip, and then observe their signal as they reach equilibrium it should be much faster for there are more possible interactions between spin-states.

4. CONCLUSION

We have shown that by applying different pulse sequences the spin-lattice relaxation time (T_1), FID time (T_2), and spin-echo decay time (T_2') were determined for different samples. By analyzing an unknown substance we related the relaxation times to other known values and determined the unknown substance to be paraffin oil or something of very similar chemical composition. In addition, comparisons between the relaxation times and amount of moles of $\text{Fe}(\text{NO}_3)_3$ in water were made. While these determinations were made lacking an ample supply of data points, our intuitions were satisfied. Overall the power of studying NMR for different samples and classifying them based upon results is shown.

5. REFERENCES

1. PHY 445. **Nuclear Magnetic Resonance (NMR)**. 2013
2. Barbara Wolff-Reichert **A Conceptual Tour of TeachSpin's pulsed NMR**. http://www.teachspin.com/instruments/pulsed_NMR/PNMR_Concept_Tour.pdf. 2003
3. **Nuclear Magnetic Resonance Manual**. Department of Physics and Astronomy. Stony Brook University.
4. John R. Taylor. **An Introduction to Error Analysis: The Study of Uncertainties in Physical Measurements Second Edition**. *University Science Books*. 1997.

6. APPENDIX

6.1. Graphs for T_1

All the fitting functions are the same as in Eq. (12).

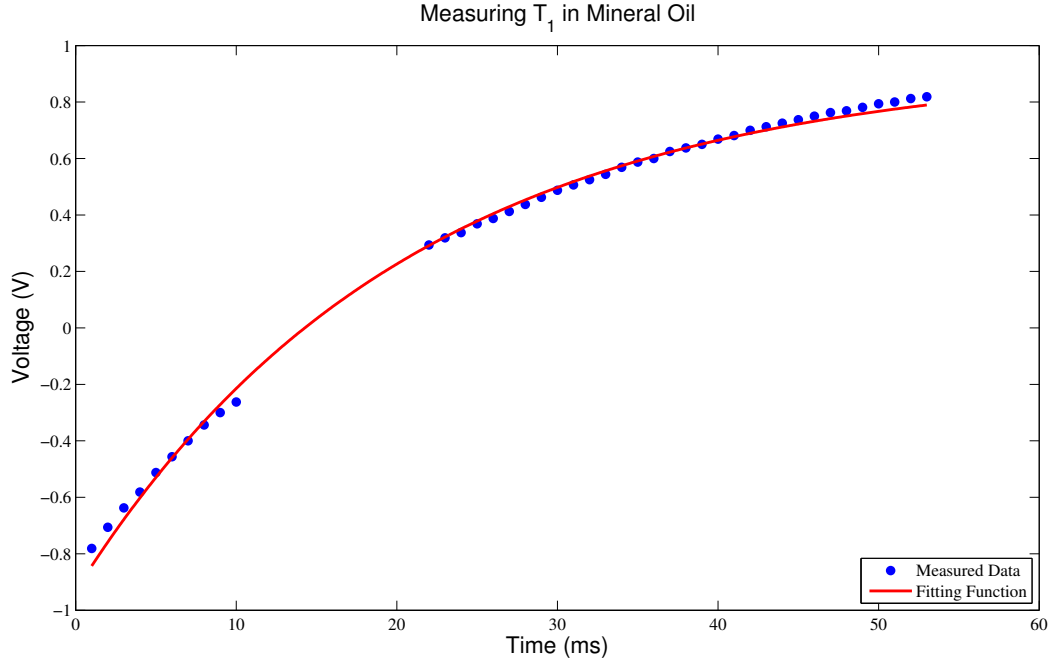


FIG. 6: We estimated that $T_1 = 20.59 \pm 0.36$ ms for a fit of $\sigma = 0.02$ and reduced $\chi^2 = 1.23$

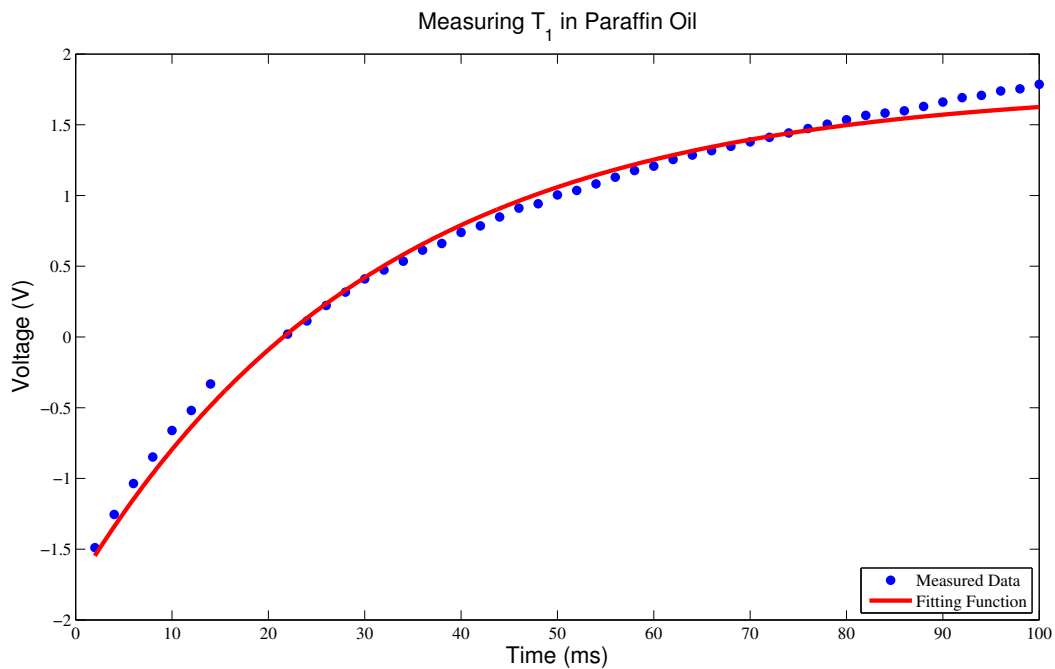


FIG. 7: Here we found that $T_1 = 31.11 \pm 0.93$ ms for a fit of $\sigma = 0.073$ and reduced $\chi^2 = 1.05$

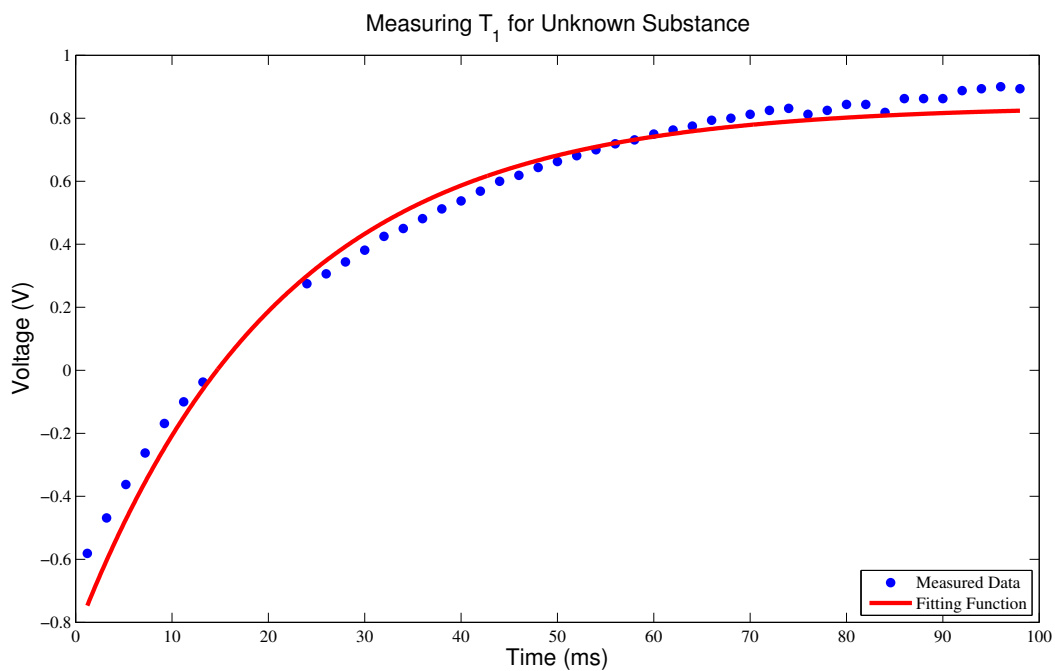


FIG. 8: We estimated that $T_1 = 21.17 \pm 1.24$ ms for a fit of $\sigma = 0.045$ and reduced $\chi^2 = 1.59$

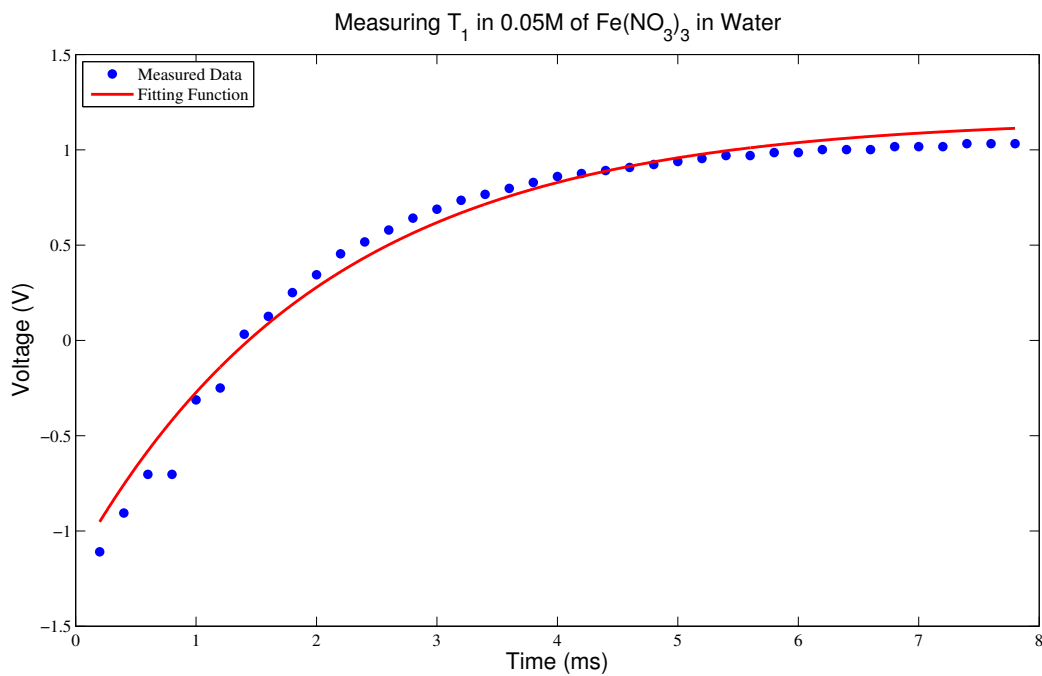


FIG. 9: Here we found that $T_1 = 2.07 \pm 0.118$ ms for a fit of $\sigma = 0.073$ and reduced $\chi^2 = 1.33$

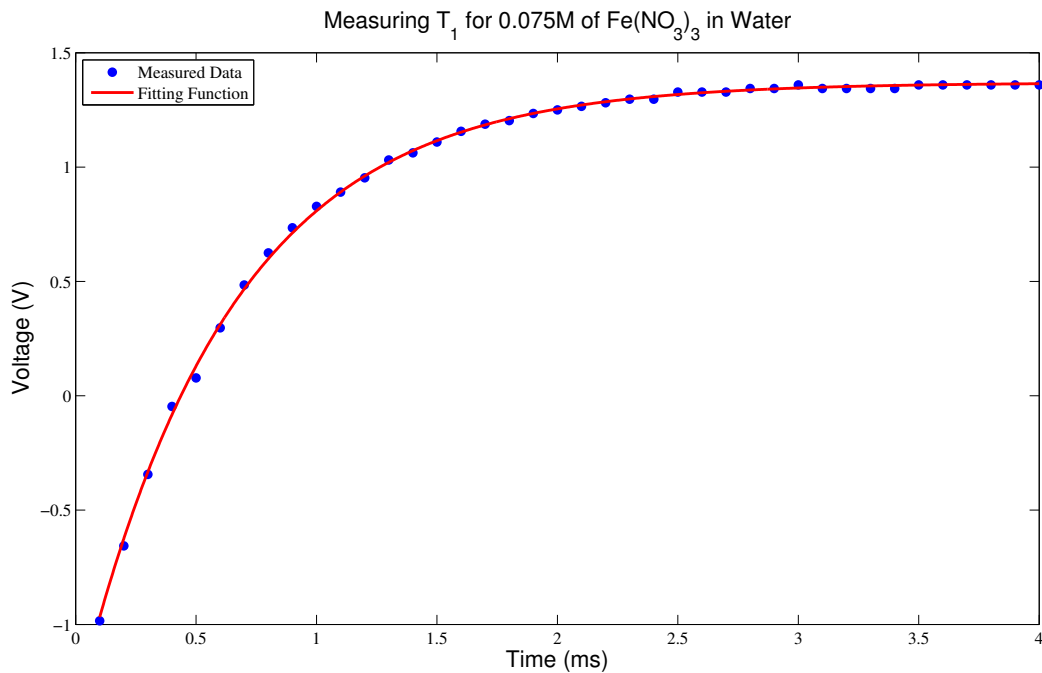


FIG. 10: We estimated that $T_1 = 0.6307 \pm 0.0064$ ms for a fit of $\sigma = 0.015$ and reduced $\chi^2 = 1.03$

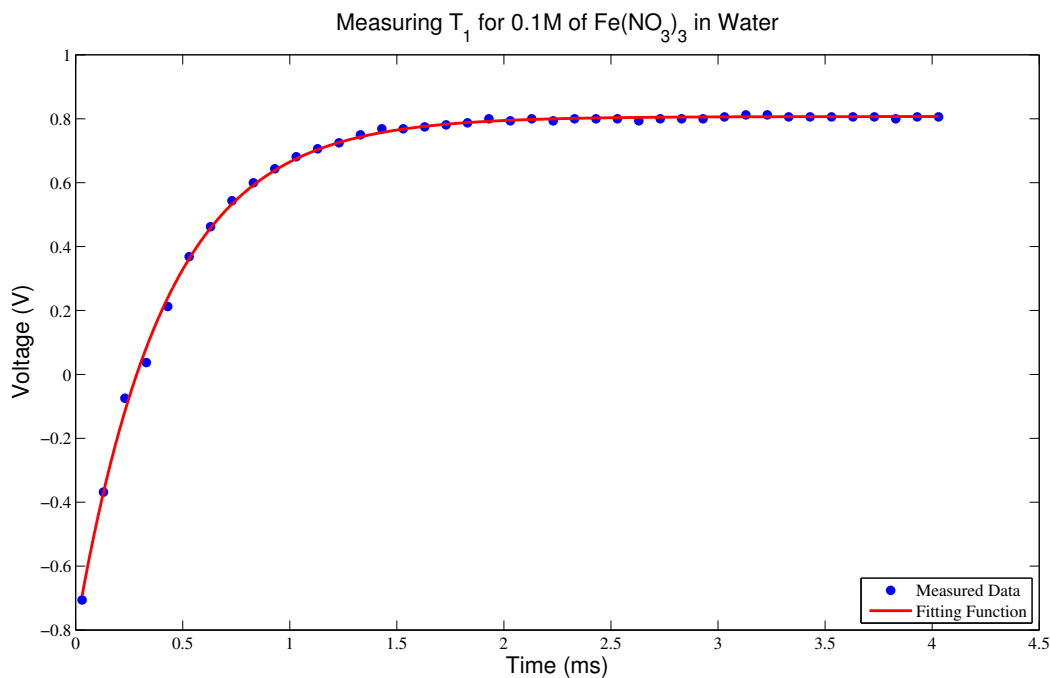


FIG. 11: Here we found that $T_1 = 0.4116 \pm 0.0065$ ms for a fit of $\sigma = 0.012$ and reduced $\chi^2 = 1.003$

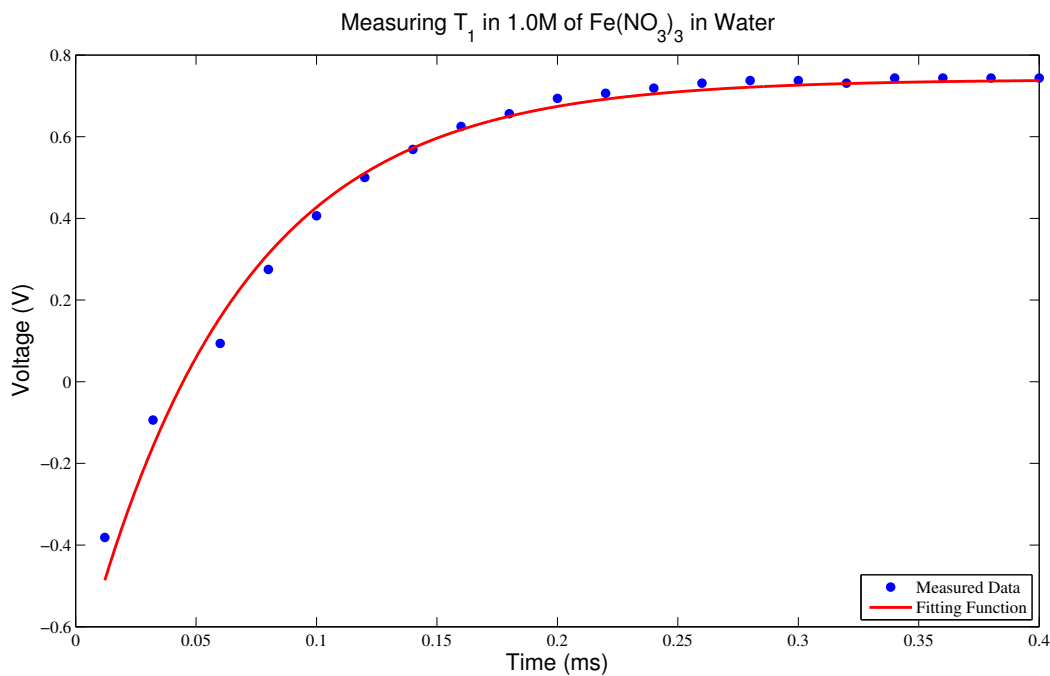


FIG. 12: We estimated that $T_1 = 0.06438 \pm 0.00429$ ms for a fit of $\sigma = 0.035$ and reduced $\chi^2 = 1.05$

6.2. Graphs for T'_2

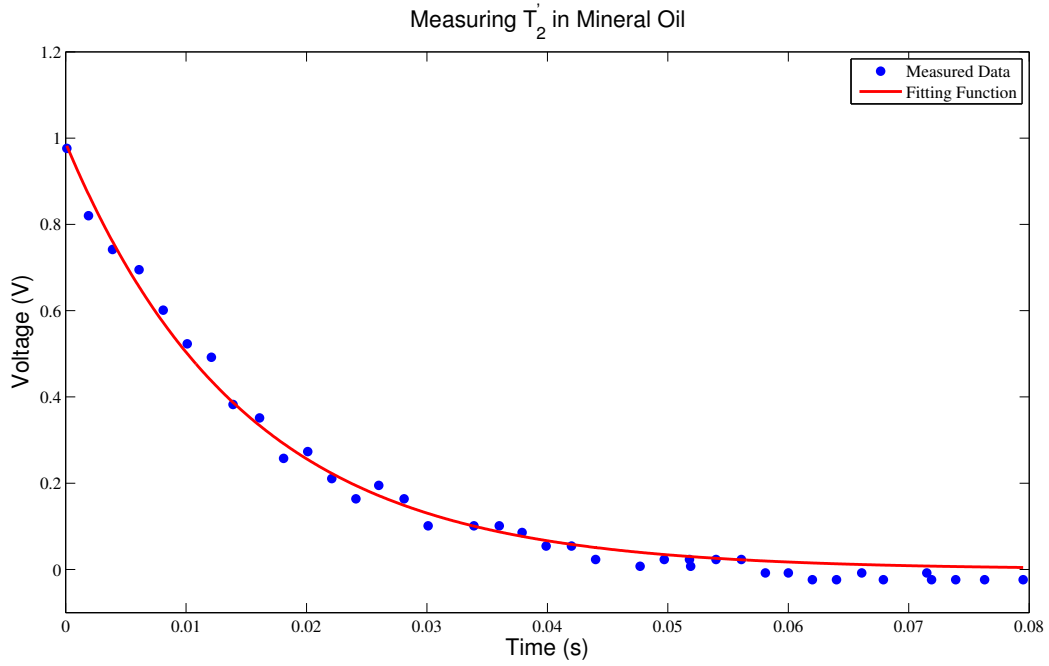


FIG. 13: Here we found that $T'_2 = 14.83 \pm 0.78$ ms for a fit of $\sigma = 0.025$ and reduced $\chi^2 = 1.09$

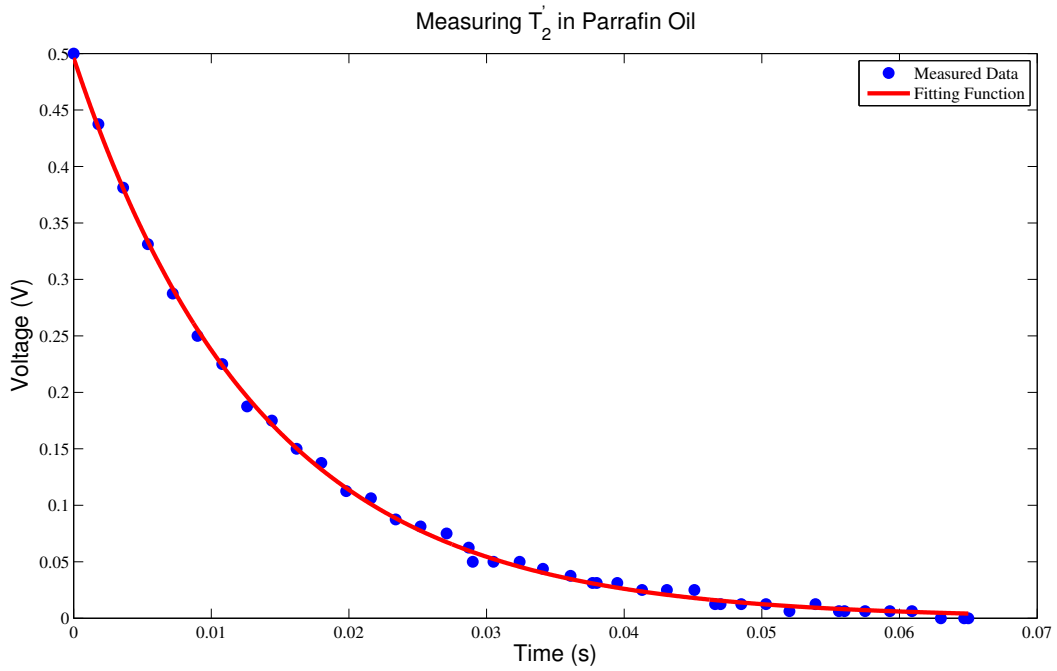


FIG. 14: Here we found that $T'_2 = 13.57 \pm 0.2$ ms for a fit of $\sigma = 0.004$ and reduced $\chi^2 = 1.08$

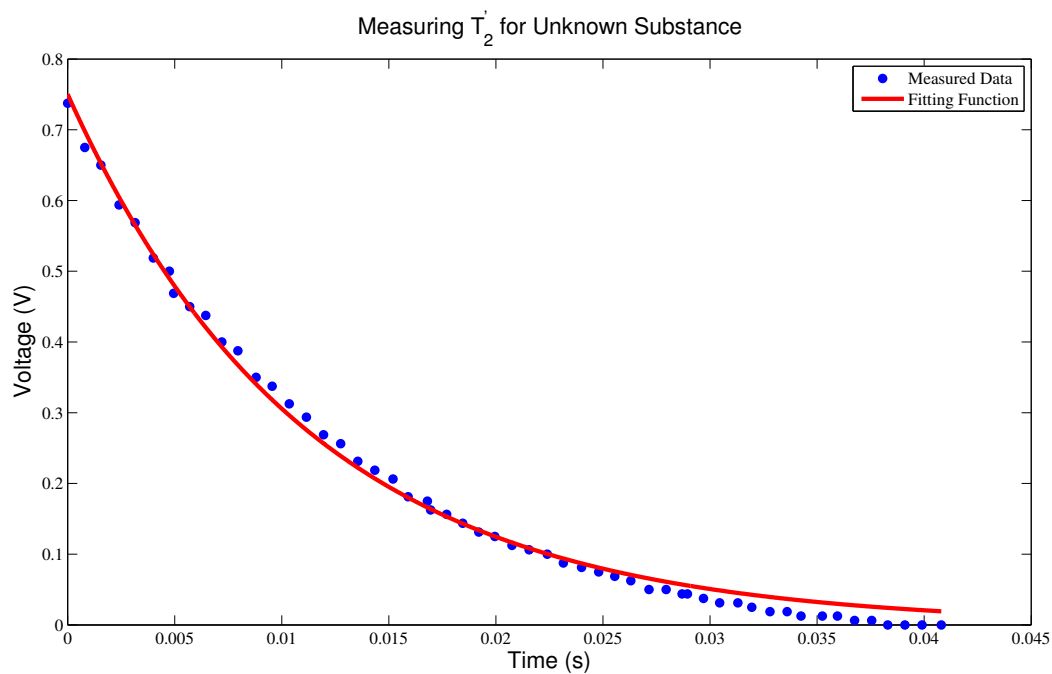


FIG. 15: Here we found that $T_2' = 11.14 \pm 0.3$ ms for a fit of $\sigma = 0.012$ and reduced $\chi^2 = 1.37$

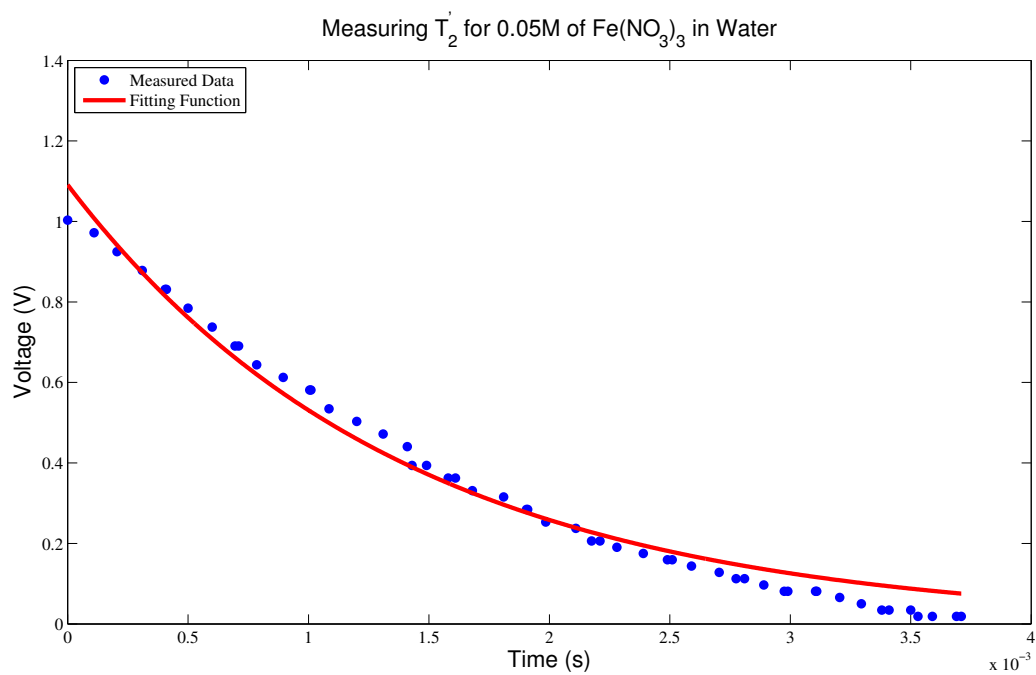


FIG. 16: Here we found that $T_2' = 1.389 \pm 0.06$ ms for a fit of $\sigma = 0.038$ and reduced $\chi^2 = 1.05$

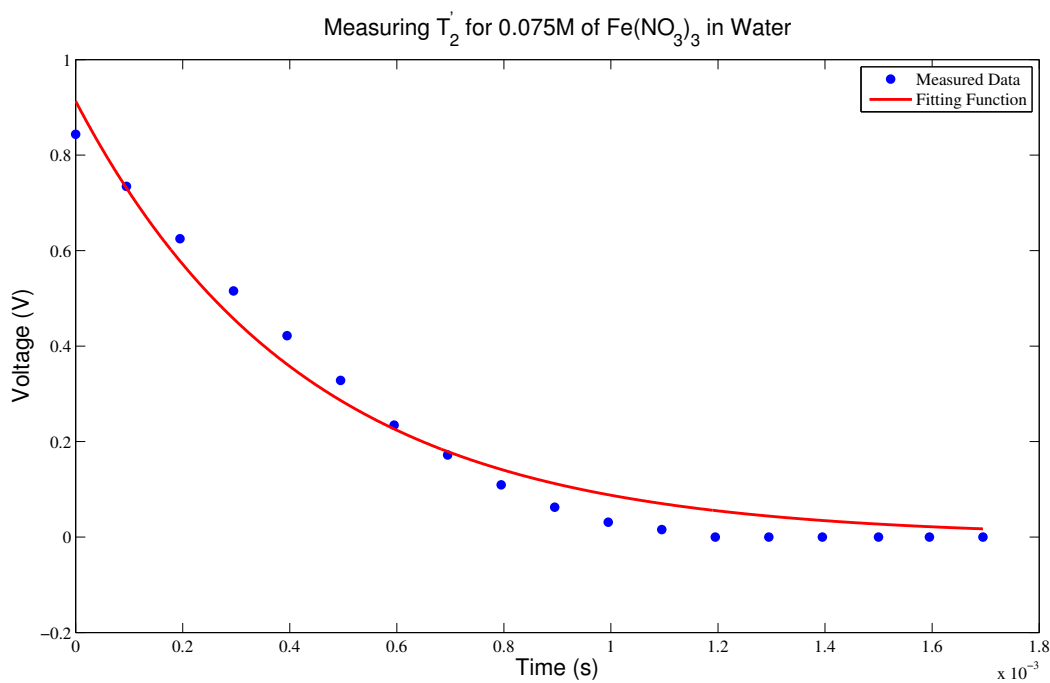


FIG. 17: Here we found that $T'_2 = 0.4266 \pm 0.0562$ ms for a fit of $\sigma = 0.04$ and reduced $\chi^2 = 1.30$

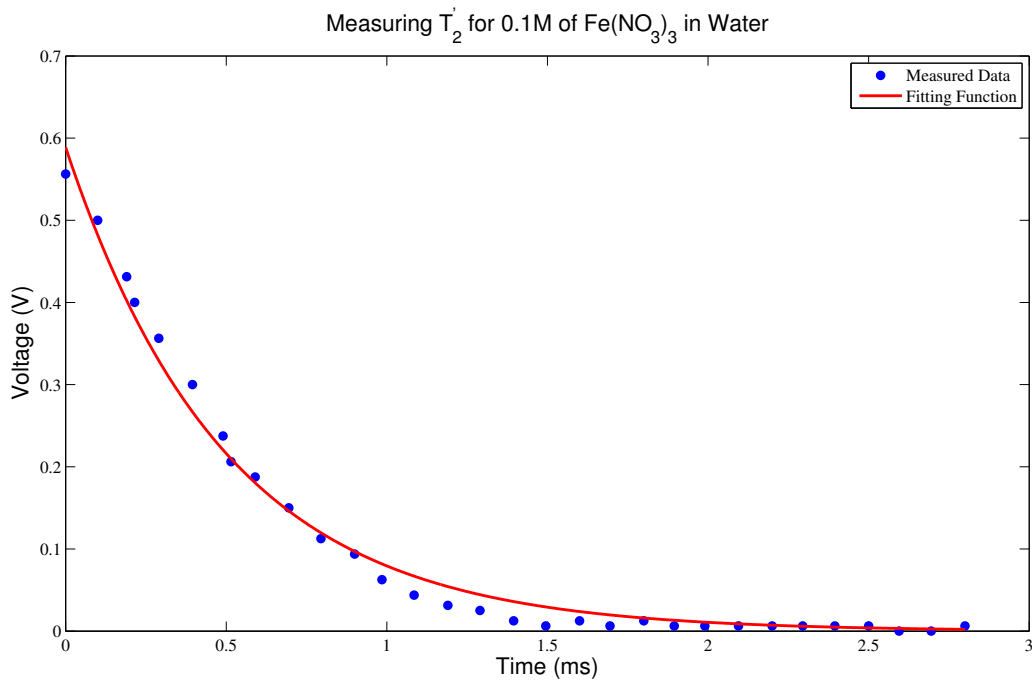


FIG. 18: Here we found that $T'_2 = 0.4989 \pm 0.0277$ ms for a fit of $\sigma = 0.0165$ and reduced $\chi^2 = 1.01$

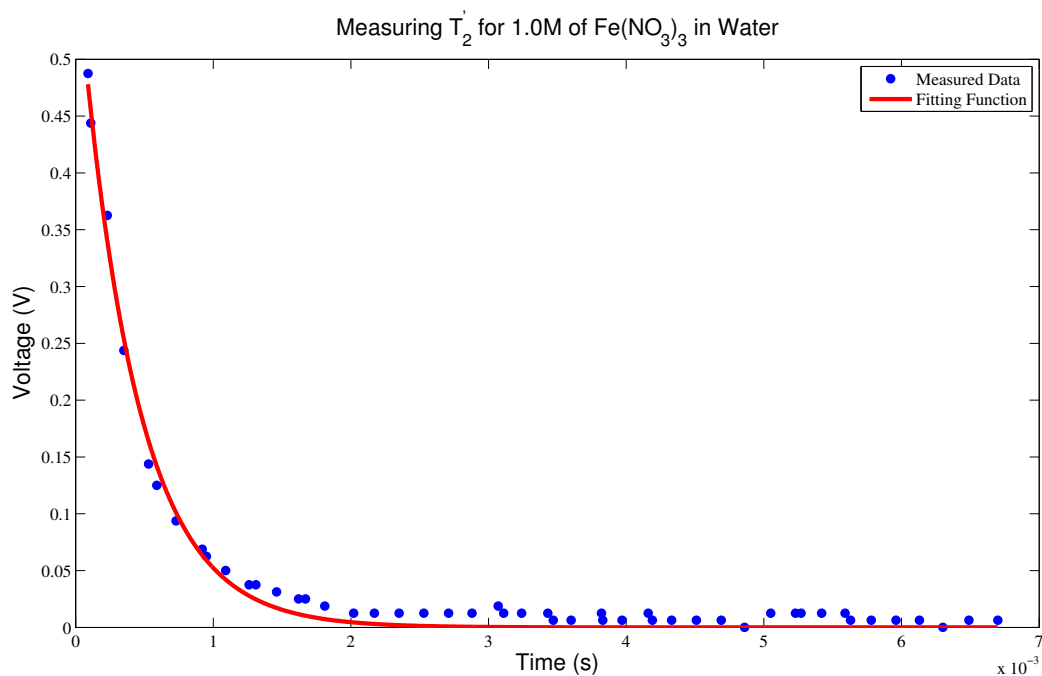


FIG. 19: Here we found that $T'_2 = 0.4116 \pm 0.0247$ ms for a fit of $\sigma = 0.0105$ and reduced $\chi^2 = 1.11$

6.3. Graphs for T_2

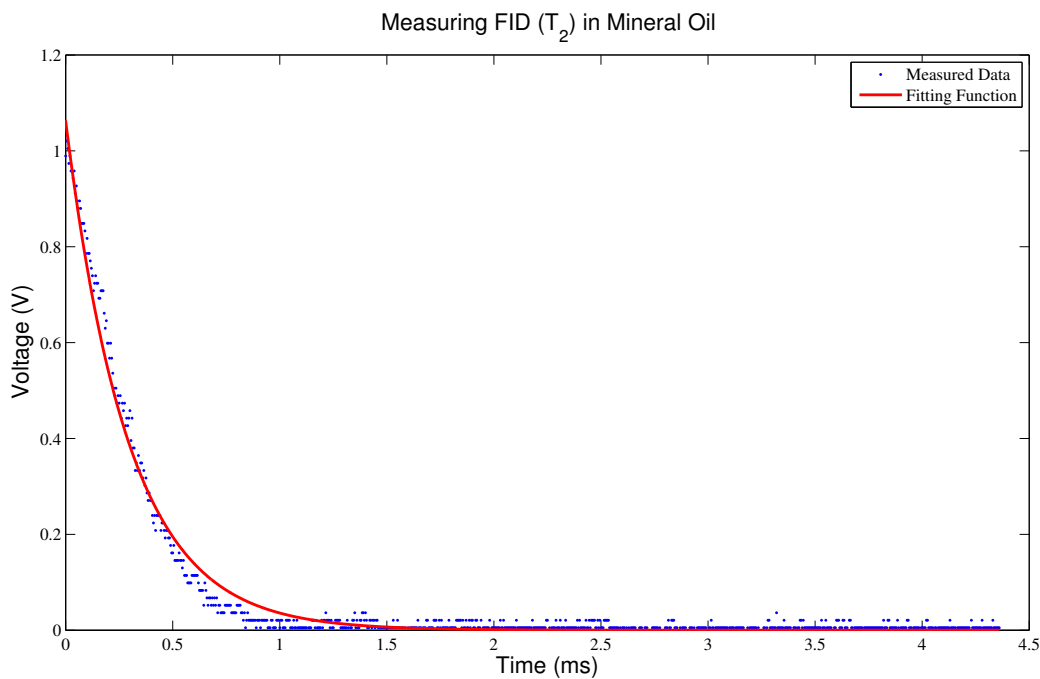


FIG. 20: Here we found that $T_2 = 0.2949 \pm 0.004$ ms for a fit of $\sigma = 0.023$ and reduced $\chi^2 = 1.03$

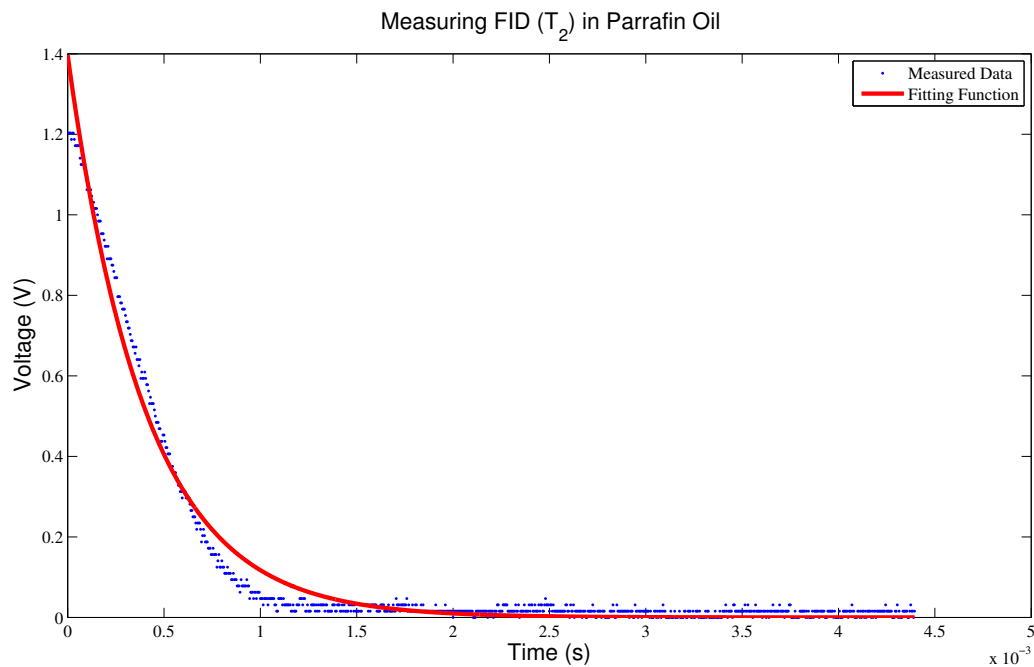


FIG. 21: Here we found that $T_2 = 0.4039 \pm 0.0063$ ms for a fit of $\sigma = 0.035$ and reduced $\chi^2 = 1.05$

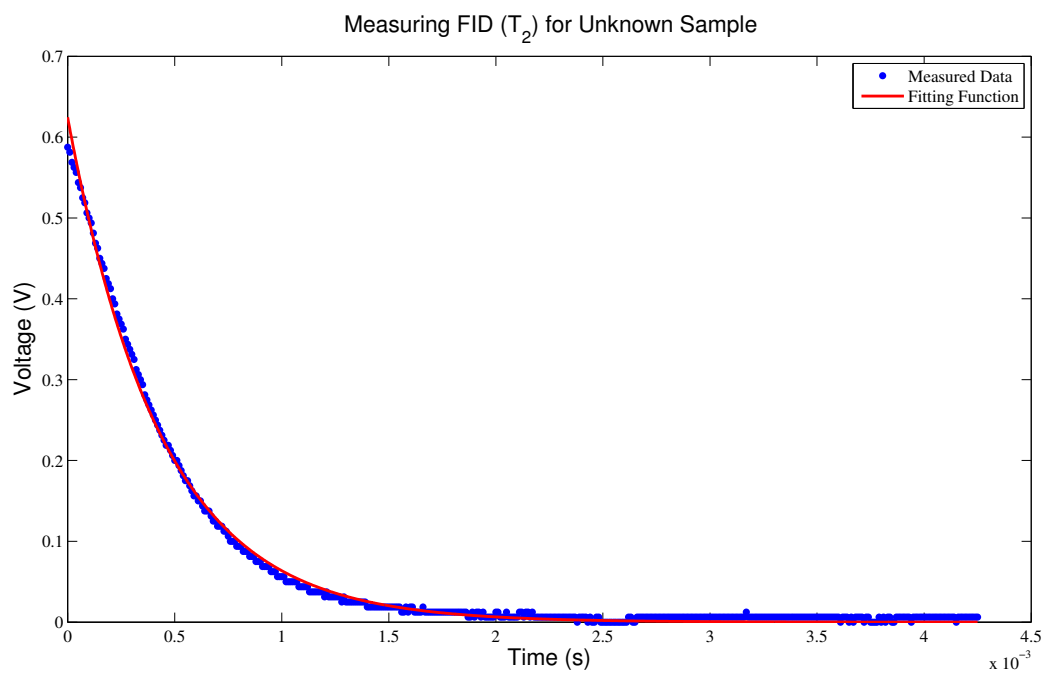


FIG. 22: Here we found that $T_2 = 0.4379 \pm 0.0038$ ms for a fit of $\sigma = 0.0065$ and reduced $\chi^2 = 1.02$

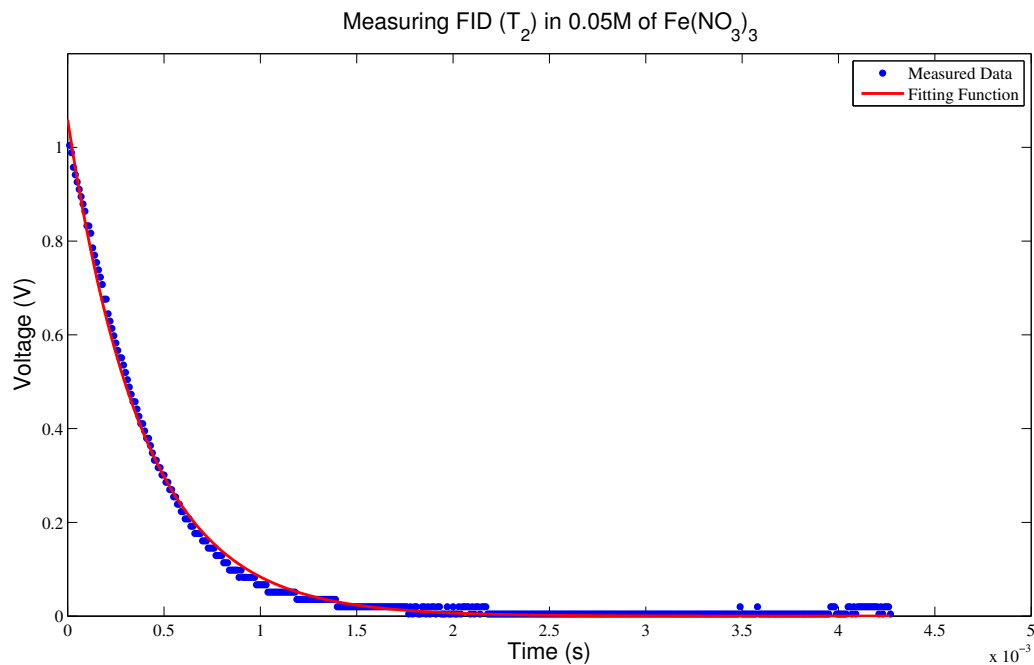


FIG. 23: Here we found that $T_2 = 0.3942 \pm 0.0039$ ms for a fit of $\sigma = 0.012$ and reduced $\chi^2 = 1.12$

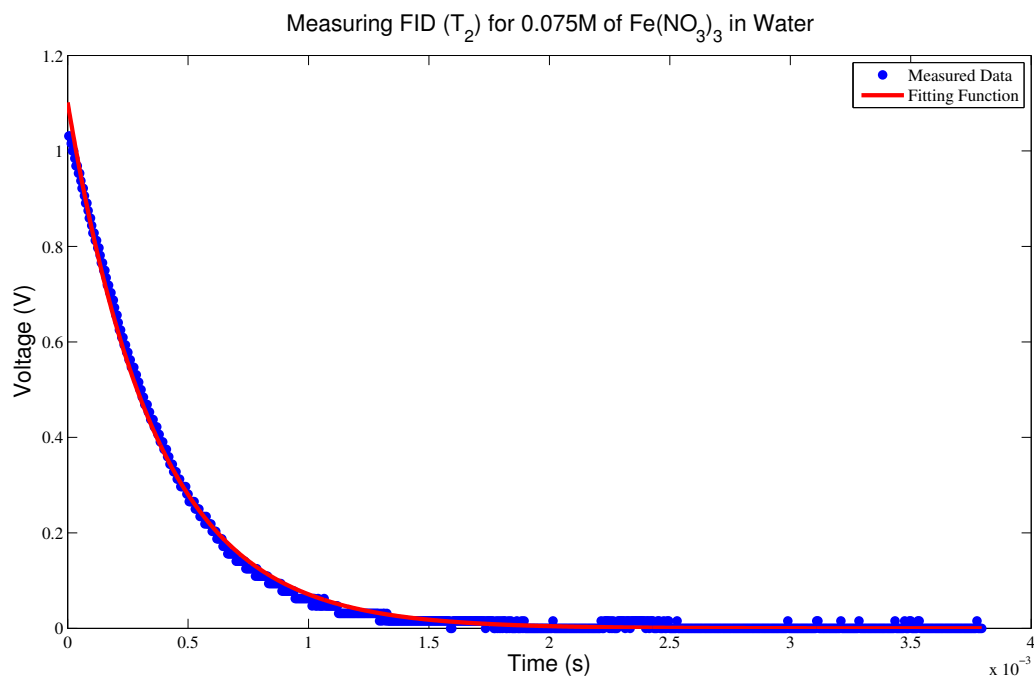


FIG. 24: Here we found that $T_2 = 0.3652 \pm 0.0021$ ms for a fit of $\sigma = 0.01$ and reduced $\chi^2 = 1.09$

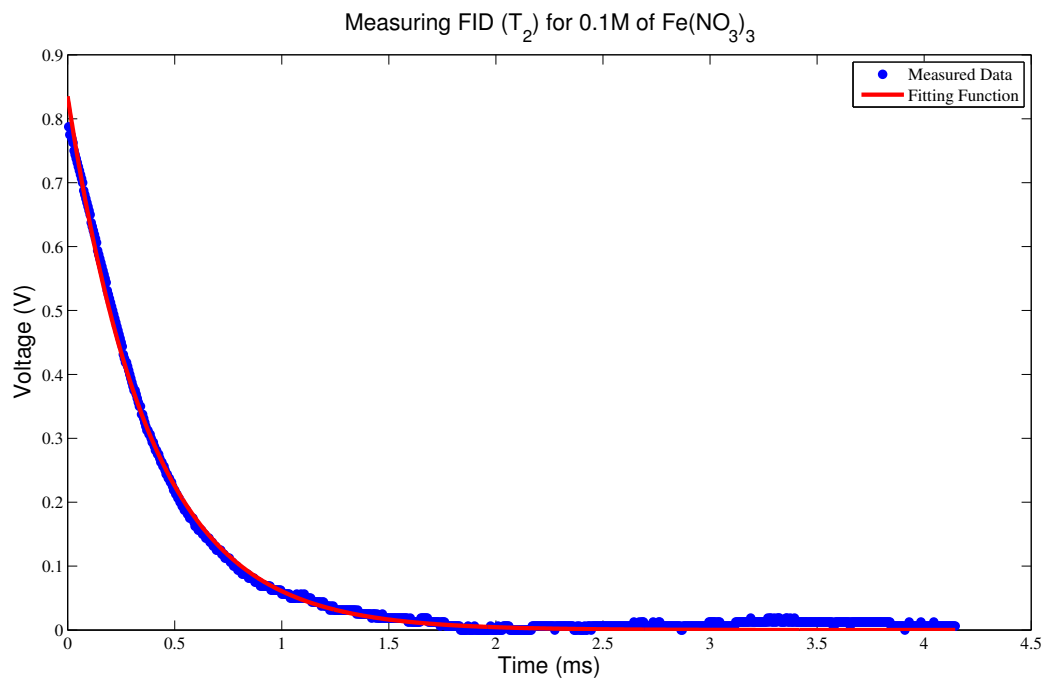


FIG. 25: Here we found that $T_2 = 0.3813 \pm 0.0025$ ms for a fit of $\sigma = 0.0085$ and reduced $\chi^2 = 1.08$

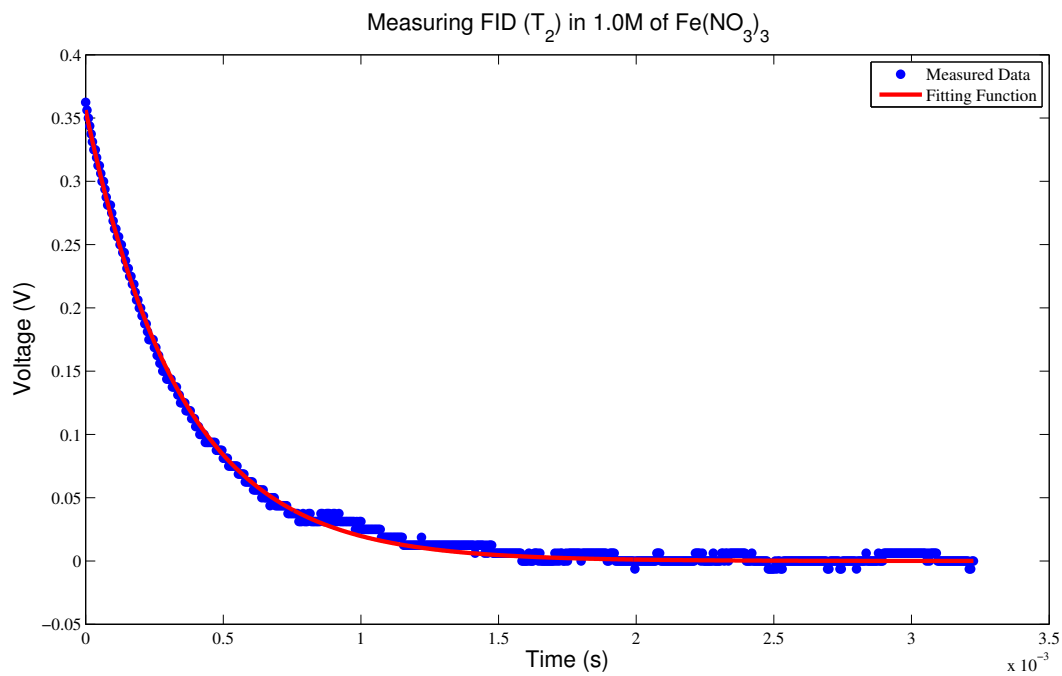


FIG. 26: Here we found that $T_2 = 0.3456 \pm 0.0027$ ms for a fit of $\sigma = 0.004$ and reduced $\chi^2 = 1.04$